ACS NANO

Cite This: ACS Nano 2019, 13, 3847−3857

www.acsnano.org

ARTICLE

Engineering Graphene Flakes for Wearable Textile Sensors *via* Highly Scalable and Ultrafast Yarn Dyeing Technique

Shaila Afroj,[†,‡] Nazmul Karim,[*,†] Zihao Wang,[‡] Sirui Tan,[§] Pei He,[§,∥] Matthew Holwill,[†,‡] Davit Ghazaryan,[‡,⊥] Anura Fernando,[§] and Kostya S. Novoselov[*,†,‡]

[†]National Graphene Institute (NGI), The University of Manchester, Booth Street East, Manchester, M13 9PL, U.K.

[‡]School of Physics & Astronomy, The University of Manchester, Oxford Road, Manchester, M13 9PL, U.K.

[§]School of Materials, The University of Manchester, Oxford Road, Manchester, M13 9PL, U.K.

[∥]School of Physics and Electronics, Central South University, Changsha 410083, China

[⊥]Department of Physics, National Research University Higher School of Economics, Moscow, 105066, Russian Federation

Supporting Information

ABSTRACT: **Multifunctional wearable e-textiles have been a focus of much attention due to their great potential for healthcare, sportswear, fitness, space, and military applications. Among them, electroconductive textile yarn shows great promise for use as next-generation flexible sensors without compromising the properties and comfort of usual textiles. However, the current manufacturing process of metal-based electroconductive textile yarn is expensive, unscalable, and environmentally unfriendly. Here we report a highly scalable and ultrafast production of graphene-based flexible, washable, and bendable wearable textile sensors. We engineer graphene flakes and their dispersions in order to select the best formulation for wearable textile application. We then use a high-speed yarn dyeing technique to dye (coat) textile yarn with graphene-based inks. Such graphene-based yarns are then integrated into a knitted structure as a flexible sensor and could send data wirelessly to a device *via* a self-powered RFID or a low-powered Bluetooth. The graphene textile sensor thus produced shows excellent temperature sensitivity, very good washability, and extremely high flexibility. Such a process could potentially be scaled up in a high-speed industrial setup to produce tonnes (∼1000 kg/h) of electroconductive textile yarns for next-generation wearable electronics applications.**

KEYWORDS: *graphene, wearables, e-textiles, graphene yarn, textile sensors, temperature monitoring*

Wearable electronics is a focal point at the moment due to its potential applications as portable, flexible, and stretchable human-interactive sensors, actuators, displays, and energy storage devices.[1−4] Smart wearable textiles have been going through significant evolutions in recent years, through the innovation of wearable electronics[5] and due to their miniaturization and the wireless revolution. This has resulted in personalized wearable garments that can interface with the human body and continuously monitor, collect, and communicate various physiological parameters such as temperature, humidity, heart rate, and activity monitoring.[6,7] Such a platform would potentially provide a solution to the overburdened healthcare system resulting from a rapidly growing aging society as well as maintaining and encouraging healthy and independent living for all, irrelevant of time and location.[8] However, current technologies for wearable garments are associated with a number of challenges that other electronic technologies do not face, such as the complex and time-consuming manufacturing process of e-textiles and the use of expensive,[9] nonbiodegradable,[10] and unstable metallic conductive materials. Apart from standard requirements for electronics and sensing capabilities, there are requirements for such e-textiles to be breathable, washable, flexible, wearable, and produced using an environmentally friendly manufacturing process.[11]

Received: January 13, 2019
Accepted: February 20, 2019
Published: February 28, 2019

DOI: 10.1021/acsnano.9b00319
ACS Nano 2019, 13, 3847−3857

The management of human body temperature to be as near the normal state (normothermia) as possible is considered to be crucial during physical activity[12] and anesthesia.[13] Otherwise, hyperthermia (body temp >37 °C) or hypothermia (body temp <36 °C) could potentially increase the chance of bleeding, adverse cardiac events, wound infections, and mortality rate, which results in increased hospital stays and inflated costs.[14−18] Therefore, it is important to monitor a patient's body temperature continuously and noninvasively to improve the neurological outcome and reduce the mortality rate.[19] Currently several techniques[20,21] and commercial products are available to monitor body temperature. However, these are usually rigid, not flexible, and not bendable.[22] There have been efforts to fabricate textile-based temperature sensors integrated into a garment without compromising the properties and comfort of the textiles.[23,24] However, these are again metal-based technologies and involve a complex manufacturing process of conductive textiles with poor performance. Therefore, there remains a need for conductive materials that could be used to manufacture environmentally friendly, wearable, and breathable textile-based temperature sensors.

Graphene has attracted significant research interest for wearable electronics applications due to its outstanding electrical, mechanical, and thermal properties[25−27] and its ability to act as a very good platform for both interconnects and active devices (transistors and sensors).[26] Moreover, graphene has superior thermal conductivity compared with metals and carbon nanotubes (CNTs)[28] and demonstrates the potential to circumvent the self-heating problems of electronic devices at elevated temperature.[29] Reduced graphene oxide (rGO), a form of graphene, can be produced in scalable quantities in a stable dispersion.[6,7] Recent studies[4,6,7,30,31] have highlighted the use of rGO for wearable e-textiles applications, due to its ability to interact with oxygen-containing groups in textile fibers. It would therefore become part of the textiles rather than forming only a surface coating.[4] However, challenges with the reported techniques are a multistage and time-consuming process,[7,30] a higher temperature treatment of heat-sensitive textiles, and toxic reducing agents.[31] Several studies reported graphene-based temperature sensors from CVD graphene on Si/SiO_2 substrates,[32] a gold-doped graphene-based electrochemical device,[33] solar exfoliated reduced graphene oxide on polyimide substrates,[13] graphene−graphene oxide (GO) hybrid films,[29] and CVD graphene-assisted microfibers.[34] However, these are not flexible, washable, and bendable and are not suitable for wearable electronics applications.

Here, we report a highly scalable and ultrafast yarn dyeing technique for the production of rGO-coated textile yarns and the use of those yarns as flexible textile sensors. First, a range of graphene materials such as reduced graphene oxides and graphene flakes (G) were synthesized using rapid and environmentally friendly processes. In order to observe the temperature sensitivity, the temperature dependence of the resistance for individual rGO flakes, overlapping rGO flakes, drop-casted rGO films, and free-standing rGO-coated yarns was tested. Moreover, the use of a highly scalable yarn dyeing technique was demonstrated by producing a batch of flexible, washable, and bendable rGO-coated yarns. Such a manufacturing technique could potentially be scaled up to produce tonnes of electroconductive graphene-based yarns using existing textile machineries and without adding extra capital or production cost. The coated (dyed) yarns were then integrated into a textile structure by the most commonly used knitting technique and could be connected to a self-powered radio frequency identification (RFID) tag or a low-powered Bluetooth device. Such graphene-based yarns could also potentially be used as various sensors in order to monitor the physiological conditions of a human body without compromising the comfort and wearability of smart textiles.

RESULTS AND DISCUSSION

Engineering Graphene Flakes for Wearable Sensors.

rGO-based wearable e-textiles are of great interest due to their ability to create hydrogen or covalent bonds with cellulosic textile fibers,[4] ultimately contributing to the improved durability and washability of the final product. Moreover, rGO provides superior dispersibility in polar solvents compared with graphene,[35] due to the presence of residual functional groups even after reduction. The dispersibility of rGO could be improved by introducing an energy barrier to aggregation, through either covalent or noncovalent interactions.[36] Here, we engineer the formulation and reduction conditions of rGO flakes. We then use them as a temperature sensor platform to manufacture graphene-based wearable textiles sensors in a scalable quantity. Graphene oxide (GO) was synthesized using a modified Hummers method[37] and chemically reduced to rGO by modifying our previously reported methods.[6,7] We used ascorbic acid (AA)[38] and sodium hydrosulfite (SH)[6] as reducing agents and optimized reduction conditions, *i.e.*, time and temperature. The surface of rGO flakes was functionalized using PSS/PVA to have better dispersibility and prevent agglomeration.[39] To compare the performance, graphene-based inks were also exfoliated using a highly scalable microfluidization technique.[40,41] We used sodium dexoycholate (SDC) as a surfactant in order to disperse G flakes in water through noncovalent bonding.[42]

To prove that our inks are fundamentally suitable for temperature-sensing applications, we demonstrate the temperature dependence of the conductance of the individual monolayer flakes. Figure 1a shows the temperature dependence of the conductance of single-layer rGO (SH) flake (olive) and the corresponding optical image of the device (top inset). In the measured temperature range, the conductivity could be seen to follow exponential behavior for a single-layer rGO flake unlike the well-established model of standard variable range hopping.[43,44] To model rGO inks (where multiple flakes overlap), we also measured the temperature dependence of the conductance of the double-layer rGO structure with two rGO monolayers partly overlapping each other (bottom inset to Figure 1a). The corresponding temperature dependence, measured through the overlapping region of the double layer structure, is shown by red squares in Figure 1a. Similar to the single layer of the rGO, the temperature dependence of the flake consisting of overlapping double layers follows similar exponential dependence although with different characteristic temperature T_o and conductance G_o, Figure 1a. This suggests that one indeed can use rGO inks for temperature-sensing applications, and the temperature sensitivity will be determined largely by the conductivity of individual flakes, rather than by the transport between flakes.

In order to check the temperature dependence of the ink, we drop-casted rGO on the Si/SiO_2 wafer and performed two-probe measurements of the conductance in the range of 150 to 300 K in order to test if the obtained temperature dependence is preserved for the "multiple overlapping" flakes obtained from

DOI: 10.1021/acsnano.9b00319
ACS Nano 2019, 13, 3847−3857

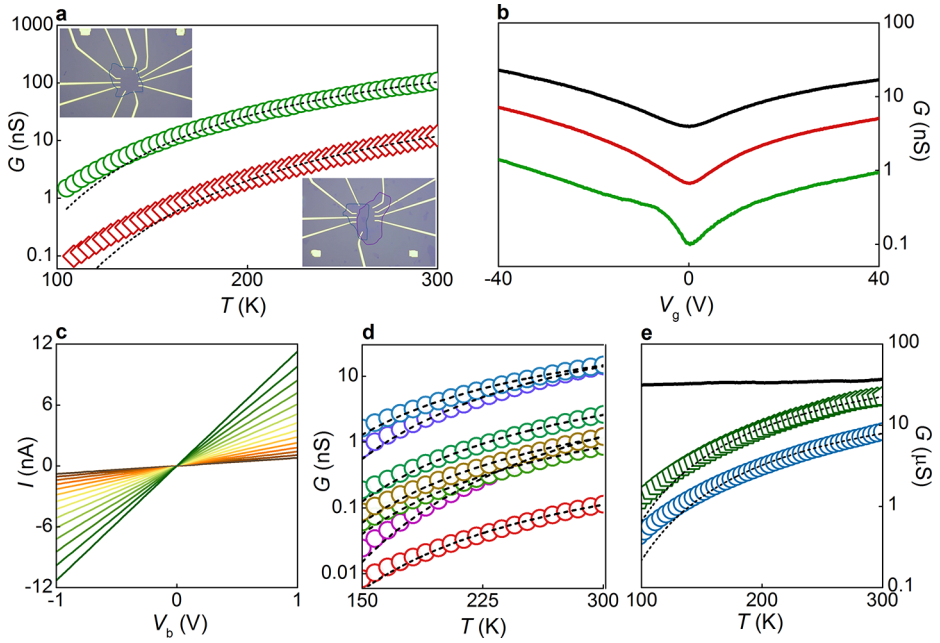

Figure 1. Electrical transport measurements from monolayer graphene flake to e-textile yarn. (a) Low bias temperature dependence of the conductance of Si/SiO_2-supported single- (olive) and double-layer overlapping (red) flakes of rGO (SH) and corresponding fittings (black dashed lines, exponential dependence, Table S2 of Supporting Information). The insets show micrographs of the devices. (b) Gate dependence of the resistance of a single-layer flake of rGO (SH) presented in (a) at temperatures of 300 K (black), 200 K (red), and 100 K (olive). (c) Example temperature dependence of *I*−*V* characteristics of rGO (SH) with a reduction time of 24 h and 1:5 GO to PSS polymer ratio (color scale for temperature from 150 to 300 K). (d) Low bias temperature dependence of conductance of Si/SiO_2-supported rGO (SH) ink droplets of 1:5 (top three lines) and 1:10 (bottom four lines) polymer/material ratio and reducing time shown in Table S2, Supporting Information. The black dashed lines correspond to the exponential fittings (Table S2). (e) Low bias temperature dependence of conductance of graphene yarns: coated with rGO (SH) (olive), rGO (AA) (blue), and G flakes (black). The black dashed lines correspond to the fittings of exponential dependence (Table S2).

the drop-casting. Figure 1c demonstrates an example of the *I*−*V* characteristics, measured in the range of 150 to 300 K for the particular rGO sample with the SH reducing agent, reduction time of 24 h, and 1:5 GO to PSS polymer ratio. Figure 1d shows the extracted temperature dependence of the conductance of the zero-bias conductivity of drop-casted rGO (SH) devices, which also follows the exponential dependence of $\sim\exp(-{}^{T_0}/_{T})$ for all the devices tested, but with different characteristic parameters of temperature, T_o, and conductance, G_o. We then performed the temperature dependence measurements of two-probe conductance for rGO (SH), rGO (AA), and G flakes-coated yarn, Figure 1e, and obtained a similar dependence to that for the samples drop-casted on a Si/SiO_2 substrate.

Now, as we proved that our rGO suspensions can in principle be used for temperature-sensing applications, we focus on the optimization of the inks in terms of their temperature response as well as manufacturability. We characterized the morphology of the graphene materials, and the optical images show that the mean lateral dimensions of GO, rGO (AA), rGO (SH), and G flakes are ∼5.85, ∼4.36, ∼4.86, and ∼1.45 μm, respectively (Supporting Information, Figure S2). The statistical analysis of atomic force microscopy (AFM) images reveals that the average flake thickness (*h*) of GO, rGO (AA), and rGO (SH) is ∼2.07, ∼2.27, and ∼2.21 nm, respectively (Supporting Information, Figure S3), whereas we obtain few-layer graphene by microfluidization, as 20% of G flakes are <10 nm in thickness. The Raman spectra of G flakes show a characteristic D peak at ∼1350 cm^{-1}, G peak at ∼1582 cm^{-1}, and an asymmetric 2D band at ∼2730 cm^{-1} (Supporting Information, Figure S4),[45] whereas D and G peaks are prominent for GO and rGO. The intensity ratio of the D and G band (I_D/I_G) increased after reduction from GO to rGO, Table S1, indicating the generation of a large number of sp^2 domains.[46] Moreover, X-ray photoelectron spectroscopy (XPS) analysis shows that the C/O ratio is found to be the highest for G flakes (∼24.84), as expected, and increased up to ∼6.6 (for rGO) from ∼2.4 (GO) as the oxygen content decreases after reduction.

We synthesized a range of graphene materials in order to find the best formulation for textile temperature sensor applications. We made 48 formulations in order to optimize the GO reduction for both AA and SH using various reduction times (12, 24, 48, 72 h) and four stoichiometric ratios (1:0, 1:1, 1:5, and 1:10) between GO and polymers (PSS/PVA). Figures S5−S7 show the aggregation of rGO flakes without or with a very small amount of polymer (1:0 and 1:1). However, the addition of polymers (1:5 and 1:10 ratios) significantly improves the dispersibility of rGO.[6] Figure 2a,b show that T_o decreases with an increase in reduction time for most rGO samples, which means that the conductivity increases with the increase of reduction time as expected. In particular, rGO (SH) samples require shorter reduction time to achieve higher conductivity (Table S2, Supporting Information). Moreover, the higher intensity ratio of D to G band (I_D/I_G) from Raman spectra and C/O ratio from XPS analysis indicates better reduction with SH. These results are in good agreement with conductivity results as the highest I_D/I_G (∼1.73) and C/O (∼6.59) achieved for rGO (SH) samples with 1:10 ratio and 24 h reduction times. In addition, Figure 2d,e show that rGO

DOI: 10.1021/acsnano.9b00319
ACS Nano 2019, 13, 3847−3857

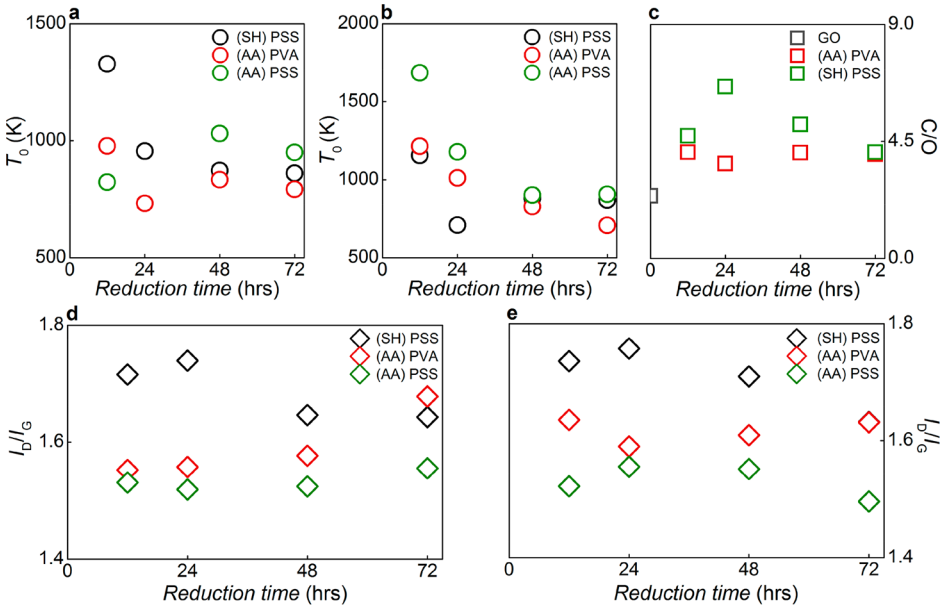

Figure 2. Optimization of rGO reduction conditions. (a) Reduction time dependence on the characteristic temperature T_0 of the conductivity of rGO inks drop-casted on Si/SiO_2 (1:5 GO/polymer ratio). (b) Reduction time dependence on the characteristic temperature T_0 of conductivity of rGO inks drop-casted on Si/SiO_2 (1:10 GO/polymer ratio). (c) Reduction time dependence on C/O ratio obtained from wide scan XPS spectra. (d) Change of intensity ratio of D to G band (I_D/I_G) of rGO flakes obtained from Raman spectra of (a). (e) Change of intensity ratio of D to G band (I_D/I_G) of rGO flakes obtained from Raman spectra of (b).

(SH) samples achieve higher I_D/I_G and C/O ratios and also require a shorter reduction time than that of rGO (AA) samples, due to the generation of a large number of sp^2 domains. This could be due to the mild reductive ability of L-ascorbic acid that takes a longer time to restore the electronics conjugation state.[47] Unlike L-AA, SH decomposes rapidly in aqueous solution at higher temperature and attacks epoxide and hydroxyl groups of GO to form rGO by hydrothermal reaction. Moreover, the color of the GO dispersion changes to black immediately after adding SH, which also demonstrates a better reduction ability of SH than L-AA.[6,48]

Ultrafast Yarn Dyeing of Highly Washable and Ultraflexible Graphene Yarn. One of the major challenges for wearable e-textile fabrication is the ability to produce conductive textiles in scalable quantities. We have addressed this to some extent in our previous study[6] on the scalable production of graphene-based conductive fabrics with the potential to produce graphene e-textiles at commercial production rates of ~150 m/min. However, it is also desirable to produce conductive textile yarn (rather than fabric) and then integrate such yarns into a fabric structure by knitting, weaving, or embroidery. The textiles sensors thus produced achieve better comfort, mobility, usability, and aesthetic properties.[49,50] Moreover, the process will provide the flexibility of producing sensors with preferred designs, structures, and properties.[51] However, further development is necessary, as current metal-based or other technologies to produce conductive yarn are neither scalable and durable nor flexible.[49,51,52]

Here we report a highly scalable and ultrafast yarn dyeing technique to produce graphene-based conductive yarn in a scalable quantity for textile sensor applications. At first, we used a simple dip-coating technique to optimize the coating time, number of coating cycles, and curing time and temperature for rGO-coated conductive yarn, Figure 3. Figure 3a shows that the resistance per cm of rGO (SH)-coated yarn decreases rapidly with the increase of coating time. We used 30 min as an optimized coating time in order to observe the effect of the number of coating cycles on the resistance of conductive textile yarn. Note that all the samples were dried at 100 °C after each coating cycle. As expected, the resistance of conductive yarn decreases with the increase in number of coating cycles due to the deposition of an increased amount of rGO flakes on the yarn surface.[6] The resistance decreases rapidly up to 3 coating cycles to ~42.7 kΩ/cm, and there are very small changes with a further coating, Figure 3b. This may be due to the absorption of a significant amount of rGO flakes into surface-pretreated 100% cotton yarns during the first 3 coating (dyeing) cycles. After that, it may almost reach a saturation point, and the resistance of the coated yarn slightly decreases with the increase of the number of coating cycles. Considering the trade-off between the conductivity and coating cycle number, we use 3 cycles of rGO coating for subsequent experiments.

Figure 3c shows the effect of curing conditions on the resistance of rGO-coated yarn and demonstrates the significant effect of curing temperature and time on the conductivity of coated yarn. The resistance decreases significantly with the increase in curing temperature and time due to the volatilization of the residual solvent.[53] Moreover, the efficient charge transport is achieved at a higher temperature by reducing the contact resistance through the rGO flake network. However, the strength of the cotton fiber decreases significantly at a higher curing temperature (above 140 °C) due to the intramacromolecular cross-linking and depolymerization of cellulose.[54] On the basis of our previous study and the usual curing temperature for fabric finishing or dyeing or printing,[55] we have chosen 150 °C for 3 min as the optimized curing conditions for the batch production of graphene-based yarn, and no significant variation in yarn strength is observed after curing. However, these problems were not addressed in previous studies on graphene-based e-textiles with a higher

DOI: 10.1021/acsnano.9b00319
ACS Nano 2019, 13, 3847−3857

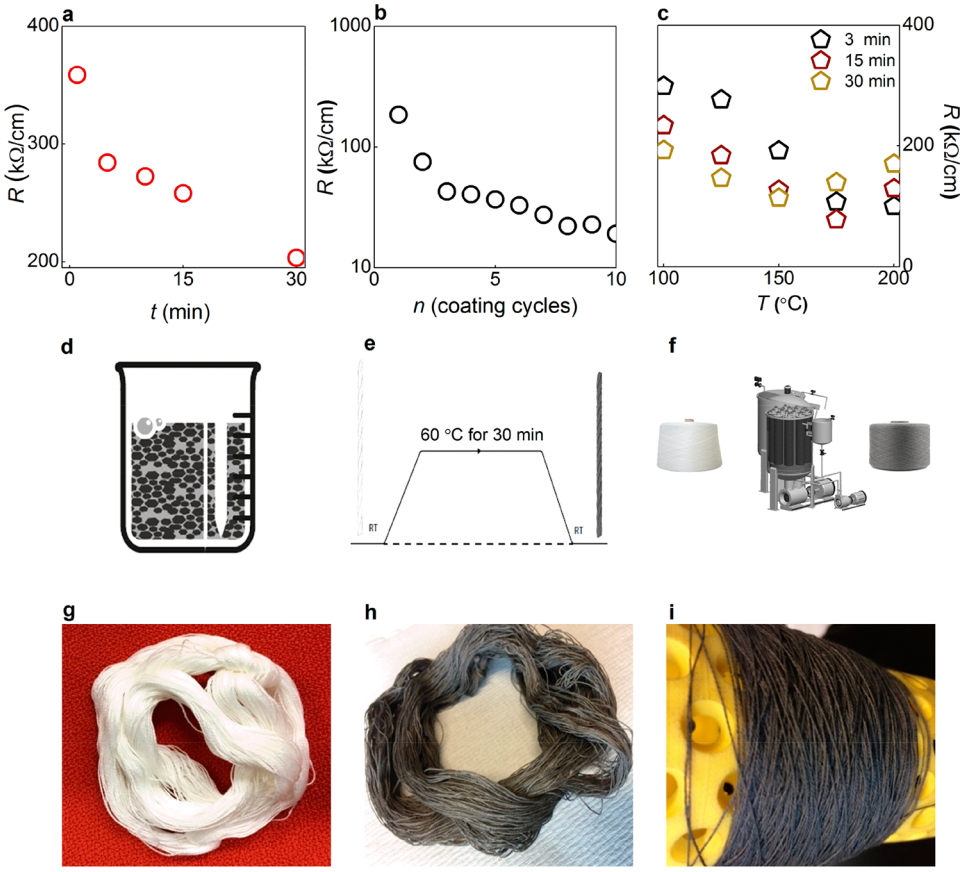

Figure 3. Optimization of rGO coating. (a) Change of resistance of rGO (SH) yarn with coating time. (b) Resistance of rGO (SH)-coated and dried (at 100 °C) yarn *vs* number of coating cycles. (c) Change of rGO (SH) yarn resistance with curing time and temperature. (d) Illustration of rapidly reduced graphene oxide rGO (SH) ink. (e) Dyeing cycle diagram of textile yarn with rGO (SH) at 60 °C for 30 min. (f) Commercial yarn dyeing machine, which could potentially dye tonnes (~1000 kg) of textile yarn (in packages). (g) Undyed hank of scoured−bleached control cotton yarn. (h) Hank of rGO-dyed (coated) cotton yarn. (i) Highly flexible graphene-coated yarn wrapped around a cone.

post-reduction temperature of GO-coated textiles or chemical reduction with a toxic reducing agent such as hydrazine hydrate and hydroiodic acid.[56,57]

In order to produce graphene-based conductive textile yarn in scalable quantity, we use a batch yarn dyeing (also referred to as "*exhaust dyeing*") technique to coat graphene onto textile yarn. The batch dyeing technique is one of the most commonly used techniques in the textile industry to dye textiles in any format such as yarn, fabric, and garments. It can dye tonnes (~1000 kg) of cotton textile yarns in just 30 min and provides even dye distribution, levelness of shade (color), and wash fastness. In this study, we mimic the batch yarn dyeing technique by coating a hank of yarn using a laboratory-scale batch dyeing machine. First, rGO (SH) ink was synthesized in a scalable quantity by reducing GO rapidly, Figure 3d. After that, a hank of cotton yarn was dyed with rGO (SH) inks by following the dyeing cycle as illustrated in Figure 3e. Such a process could potentially be scaled up with an industrial scale yarn dyeing machine, Figure 3f, and produce tonnes of graphene-based conductive yarn in a cost-effective manner. Figure 3g shows a hank of scoured−bleached 100% cotton white yarn, which is dyed (coated) with rGO in a batch dyeing machine at 60 °C for 30 min and subsequently dried at a lower drying temperature (100 °C) and cured at 150 °C for 3 min to produce conductive textile yarns, Figure 3h. Thus, produced graphene-based textile yarns are as ultraflexible (easily wrapped around a cone, Figure 3i) as untreated yarn, durable, and comfortable.

The wash stability of wearable e-textiles is extremely important for daily use. The wash stability of rGO-coated yarn was investigated and compared with that of G flakes-coated yarn. A British standard (BS EN ISO 105 C06 A1S) test procedure and SDC ECE reference detergent B that contains phosphate were used. The graphene-coated yarn was exposed to mechanical agitation (by 10 steel balls) and washing powder during a simulated home laundry wash. Our rGO-coated yarns can sustain a number of washings and are still conductive after 10 washing cycles. After each washing, the resistance of rGO-coated yarn increases slightly up to 6 cycles, Figure 4a, due to the removal of unfixed rGO flakes from the surface.[6] The SEM image of untreated cotton yarn shows smooth featureless fibers, Figure 4b. After rGO coating, the individual fibers are wrapped with rGO flakes with a very uniform coating, Figure 4c. Moreover, it is difficult to distinguish rGO flakes from the fiber unless there are unfixed rGO flakes on the fiber surface due to defects in coating, Figure 4d. These unfixed flakes are removed during washing cycles (Supporting Information, Figure S16b) and possibly increase the resistance of rGO-coated yarns after each washing cycle. However, the wash stability could further be increased by a fine encapsulation layer on the yarn surface. Unlike rGO yarns, the wash stability of G-coated yarn is found to be very poor, as the

DOI: 10.1021/acsnano.9b00319
ACS Nano 2019, 13, 3847−3857

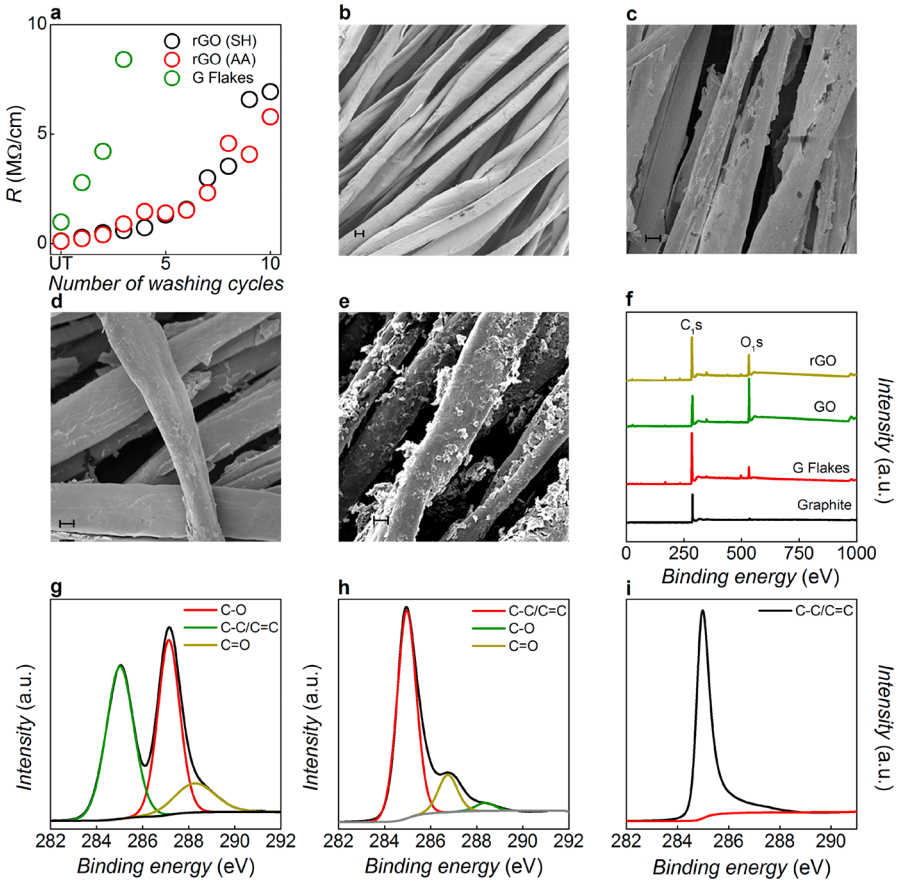

Figure 4. Wash stability and durability of coated yarn. (a) Change of resistance of graphene-coated yarn with number of washing cycles. (b) SEM image of untreated control yarn (×500). (c) SEM image of rGO (SH)-dyed (coated) cotton yarn (×1000). (d) SEM image of rGO (SH)-dyed (coated) cotton yarn (×2000). (e) SEM image of G flakes-dyed (coated) cotton yarn (×1000). (f) Wide-scan XPS spectra of graphite, G flakes, GO, and rGO. (g) High-resolution C (1s) XPS spectrum of GO. (h) High-resolution C (1s) XPS spectrum of rGO. (i) High-resolution C (1s) XPS spectrum of G flakes. All the scale bar on SEM images are 5 μm.

resistance increases rapidly after each wash. It loses electrical conductivity after 3 washing cycles, due to the removal of G flakes from the yarn surface, Figure 4a. SEM images of G-coated yarn show that a large number of G flakes are loosely attached to the fiber surfaces (Figure 4e), which were removed during the mechanical agitation created by washing (Supporting Information, Figure S16c,d).

XPS analyses of rGO and G inks provide further evidence for better wash stability of rGO yarns and the poor wash stability of G yarns. As seen from the wide-scan spectra of graphene materials in Figure 4f, GO contains a significant amount of oxygen (~29.4%), which decreases with the reduction, whereas G flakes contain a very small amount of oxygen (~3.7), almost the same as graphite. High-resolution XPS analysis shows that GO contains oxygen functional groups such as C−O epoxy and alkoxy groups (~286.4 eV) and C═O carbonyl groups (~288 eV),[7] Figure 4g. After reduction to rGO, such oxygen-containing functional groups are almost diminished with a small number of residual oxygen functional groups left around 288.5 eV, Figure 4h. These residual functional groups of rGO create covalent or hydrogen bonding with the fibers and impart better wash stability. However, no such oxygen functional groups are observed in high-resolution spectra of G flakes (Figure 4i), which is mainly dominated by C−C/C═C and very similar to graphite. Therefore, G yarns provide poor wash stability.

Knitted Temperature Sensors and Characterization. An automatic knitting technique was used to provide a scaffold for the placement of the graphene-coated yarn sensor. Such automated knitting technology allows the sensor construction to be a part of the garment manufacturing process and thereby facilitates the accurate placement of any sensor geometry anywhere in the garment. Through this advanced knitting technique, the sensor manufacturing is standardized to ensure repeatability of the sensor manufacturing and thereby its performance. A knitted structure provides the base for introducing graphene yarn as a temperature sensor. In order to provide the graphene-coated temperature sensor yarn with the most stable knitted scaffold, it was constructed to have an interlock structure made of double-covered yarn with a Lycra filament core and a nylon filament covering, Figure 5a,b. The interlock structure, due to its high resistance to structural deformation, offers the best dynamically stable scaffold or background structure to carry the sensor yarn. In order to improve the sensor performance, we assembled the sensor yarn course in such a way that it contains a tubular structure with graphene yarn only on the front side of the tubular knitted courses, Figure 5b.

Since the graphene-coated yarn is a short fiber cotton yarn, if the yarn is integrated as a straight laid-in yarn, it is possible that the yarn may experience some permanent deformation during the fabric handling. Such an occurrence would have the capacity to change the yarn properties that are defined in its

DOI: 10.1021/acsnano.9b00319
ACS Nano 2019, 13, 3847−3857

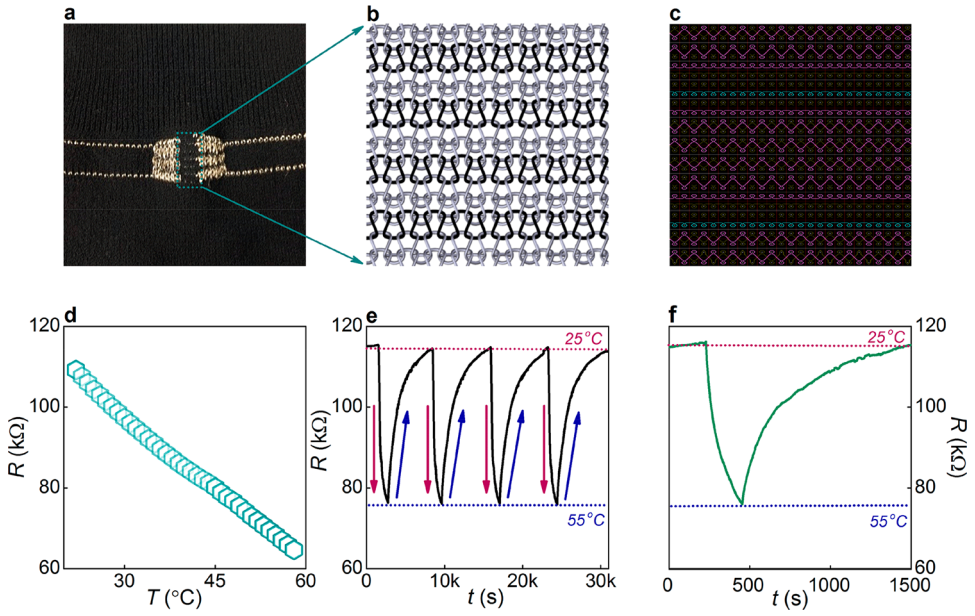

Figure 5. Fabrication and characterization of knitted graphene sensors. (a) Knitted temperature sensor with graphene-coated yarn. (b) Knitted structure used as a scaffold for the placement of graphene yarn as a temperature sensor. (c) Yarn path notation diagram for knitted temperature sensors. (d) Temperature dependence of the resistance of the knitted sensor showing almost a linear change with a negative temperature coefficient. (e) Cyclic test of the knitted sensor's temperature sensitivity between 25 and 55 °C showing excellent repeatability. (f) Time response property of the knitted temperature sensor.

electromechanical characterization. Therefore, the graphene-coated sensor yarns were introduced as a plain knitted structure, which is in effect a series of yarn loops that help to prevent any changes to the yarn properties during usage. Patches of silver yarn knitted structures were also assembled on either side of the knitted courses of graphene yarn to provide bus bars, Figure 5a. Such bus bars are in fact low-resistance electrodes for the conductive pathways to feed the electrical signals to the control unit. Figure 5c shows the yarn path notation diagram for the knitted temperature sensor, where the design repeat is from one blue knitted course to the other blue knitted course.

Figure 5d shows the temperature-sensing performance of the graphene-based knitted temperature sensor in Figure 5a. It can be seen that the resistance of this sensor is decreasing almost at a constant rate with the increase of temperature from 20 °C to around ~60 °C. The effect of the temperature on the resistance of the knitted sensor is similar to what has been observed for thermally[58] and chemically[59] reduced GO films. Figure 5e confirms a good temperature-sensing stability of this sample in a cyclic test between 25 and 55 °C. The longer time of temperature decrease from 55 °C to 25 °C is due to the slow cooling speed of the oven. Figure 5f shows the time response property of the knitted temperature sensor, when the temperature is increased from 25 °C to 55 °C by transferring the knitted sample from the oven (55 °C) to room temperature (25 °C).

Smart Wearable Garment with Ultraflexible Graphene-Based Wireless Sensors. We further investigate the flexibility of graphene-based yarns under bending and compression. Figure 6a shows a repeatable response for bending (concave downward) in forward (bending) and reverse (bending back) directions. Similarly for compression with a concave upward position, the change in resistance of the rGO yarns is repeatable in both the forward (compression) and reverse (compression back) directions (Figure 6b). Moreover, the variation in the resistance is almost stable up to 1000 bending−releasing and compression−releasing cycles, Figure 6c. Similarly, the resistance changes barely after 10 repeated folding−releasing operations (Figure 6d) when subject to the more violent deformation of folding. Moreover, excellent adhesion is observed, as no materials come off the surface of graphene-coated yarns. We do not observe creasing or a change of shape of the yarns due to these aggressive mechanical actions such as folding, bending, and compression. This demonstrates excellent flexibility of the graphene-based yarns and their great promise for wearable and bendable electronics applications.

The "zero-power" RFID technology has been the heart of passive, low-cost, and low-maintenance wireless sensors.[60] With growing applications of the Internet of Things (IoT), it is estimated that wireless sensors and actuators will account for the majority of the IoT devices, due to their ability to be self-powered while monitoring physical parameters and transmitting data.[61] RFID-based sensor networks could potentially become the ultimate sensing tool and find a plethora of applications in the future world of artificial intelligence. Here, we illustrate a concept smart garment (Figure 6e) that could be integrated with a knitted temperature sensor or other wireless sensors (such as but not limited to strain, pressure, and humidity) and an RFID tag and send the temperature data to a mobile app *via* an NFC reader. This could also be connected with a low-power Bluetooth device to transmit data to a device.

CONCLUSIONS

We report a highly scalable and ultrafast production of graphene-based textile yarns that could be used for next-generation wearable electronics applications. The graphene-based electroconductive yarns thus produced are flexible, washable, and bendable and show excellent temperature sensitivity and cyclability when integrated into a knitted textile structure. We demonstrate the potential integration of self-

DOI: 10.1021/acsnano.9b00319
ACS Nano 2019, 13, 3847−3857

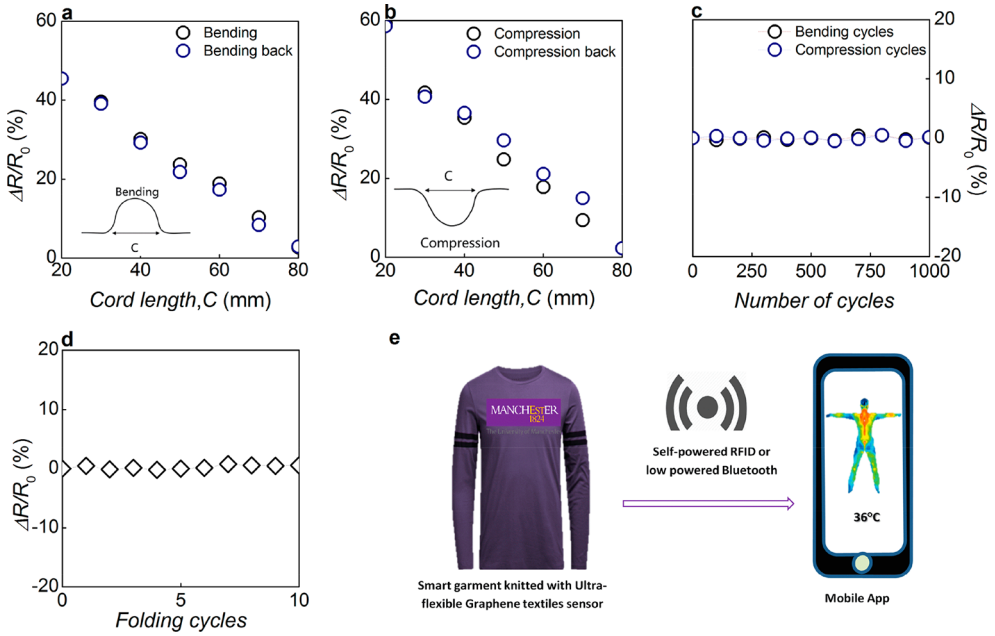

Figure 6. Graphene-based ultraflexible smart wearable e-textiles. Electrical resistance variation of graphene yarn sensors: (a) under bending: forward (bending) and reverse (bending back) directions; (b) under compression: forward (compression) and reverse (compression back) directions; (c) under cyclic bending and compression for 1000 times; and (d) performing 10 folding−releasing cycles. (e) Concept smart garment knitted with ultraflexible graphene textile sensors that would enable monitoring of physiological conditions of the human body (potentially in a hospital environment) and send data to a mobile app *via* a self-powered RFID or low-powered Bluetooth device. Illustration by Kazi Farhan Hossain Purba and used with permission from the artist and from the University of Manchester (for logo).

powered RFID with knitted temperature sensors, monitoring of human body temperature as required and sending this to a data collection unit. We believe our ultrafast production process would be an important step toward realizing multifunctional applications of wearable e-textiles for next-generation medical devices, sportswear, fashion, fitness, and military goods.

EXPERIMENTAL METHODS

Materials. Flake graphite grade 3061 and grade 2736 were kindly supplied by Asbury Graphite Mills, USA, and Graphexel Limited, UK, respectively. Poly(sodium 4-styrenesulfonate) (PSS, M_w ~70 000, powder), sodium deoxycholate (SDC), L-ascorbic acid (~99%), sodium hydrosulfite (~82%), poly(vinyl alcohol) (PVA, M_w ~31 000−50 000, 98−99%), ammonia, potassium permanganate ($KMnO_4$), sulfuric acid (H_2SO_4, ~99%), and hydrogen peroxide (H_2O_2, ~30%) were purchased from Sigma-Aldrich, UK, and used as received. Surface-pretreated (scoured and bleached) 100% cotton yarn from the University of Manchester textiles laboratory was used.

Synthesis of Graphene Materials. A modified Hummers method and microfluidization technique were used to prepare graphene oxide[37] and few-layer graphene-based inks (G flakes),[40] respectively. Our previously reported methods were modified for chemically reducing GO to rGO.[6,7] Briefly, 160 mg of GO was added to 160 mL of deionized (DI) water and sonicated for 30 min to make a 1 mg/mL brown dispersion of GO, which was transferred to a round-bottom flask placed in an oil bath. PVA and PSS polymers were added in various stoichiometric ratios (1:0, 1:1, 1:5, and 1:10) to the GO dispersion by rigorous stirring in order to make a stable dispersion. Environmentally friendly L-AA and SH (1.22 g) were used as reducing agents in order to reduce GO to rGO (SH) PSS, rGO (AA) PVA, and rGO (AA) PSS. The bath pH was maintained at 9−10 by adding a sufficient amount of ammonia solution. The mixture was then held for 12−72 h under closed conditions in order to obtain a black dispersion of rGO. This black dispersion was washed several times to remove any residuals and finally diluted into DI water to adjust the rGO dispersion concentration to ~1.9 mg/mL.

Device Fabrication and Electrical Measurements. The G and rGO flakes were drop-casted on Si/SiO_2 (290 nm oxide on plain silicon) and printed electronic paper (PEL) using a micropipet (1−10 μL) and manually bonded using silver paste for two-probe electrical characterization. The devices with single and double flakes were prepared by the usual dry transfer procedure followed by standard e-beam lithography. The electrical measurements were performed in a ^{4}He cryostat from 150 to 300 K. Source voltage was swept, and the current was measured using a Keithley 2614B source meter.

Coating and Dyeing of Textile Yarn with Graphene-Based Inks. A simple dip coating was used in order to optimize the coating and curing conditions such as coating time, number of coating cycles, curing time, and temperature. First, a scoured−bleached cotton yarn was coated with an rGO dispersion (~1.9 mg/mL) for 1−30 min, and resistance per cm length of coated yarn was measured using a multimeter (DL9309 Auto Ranging multimeter, Di-Log, UK). The optimized coating time was used to coat yarn with the same rGO dispersion for a number of coating cycles (up to 10). Then the effect of the curing time (5−30 min) and the curing temperature (100−200 °C) on the resistance of the rGO-coated yarn was observed and optimized.

In order to mimic an ultrafast and highly industrial yarn dyeing process, a laboratory scale Mathis LABOMAT dyeing machine (Werner Mathis AG, Switzerland) was used to dye (coat) ~2 g of scoured−bleached cotton yarn using a batch dyeing technique. A materials to liquor (M:L) ratio of 1:50 was used to dye a batch of cotton yarn with rGO ink at 60 °C for 30 min. The batch of dyed yarn with rGO was subsequently dried at 100 °C for 15 min.

Fabrication of Knitted Sensor and Wireless Temperature Monitoring. The fabrication of the wearable temperature sensor was accomplished using a SES-122S 10gg Shima Seiki (Japan) computer-controlled electronic flatbed knitting technology. The electro-mechanical characterization of the graphene-based knitted sensor structure was carried out using a Z/050 Zwick-Roell tensile tester (Zwick Roell Group, Germany) connected with NI-9219 National Instrument data acquisition technology (NI, American). The characterization allowed a vision into selecting the optimum knitting parameters for the sensor structure and the knowledge of the best

DOI: 10.1021/acsnano.9b00319
ACS Nano 2019, 13, 3847−3857

working region in the characteristic curve of the sensor when it is used in a wearable sensor garment.

Characterization. The graphene dispersions were diluted 1000 times and drop-casted on Si/SiO_2 (290 nm oxide on plain silicon) for flake size, flake thickness, and Raman analysis. The images and spectra were taken from 10 different locations on the sample and averages calculated. The flake size was measured using images from a high-definition optical microscope (Nikon DS−Ri2, Japan). The surface topography of the untreated and graphene materials-coated yarns was analyzed using scanning electron microscope (SEM) images from Zeiss Ultra SEM. The flake thickness of GO and rGO was measured using a Dimension Icon (Bruker) atomic force microscope. Raman spectra were collected using a Renishaw Raman System equipped with a 633 nm laser. A Kratos Axis X-ray photoelectron spectroscopy system was used to characterize the surface functionality of GO, rGO, and G flakes and also untreated and graphene-coated yarn. The wash stability of graphene material-coated cotton yarn was assessed according to BS EN ISO 105 C06 A1S as previously reported.[6]

The electrical response of the knitted temperature sensor was tested with an Ivium portable electrochemical interface and impedance analyzer (USA). An oven was used to control the temperature of the knitted sample, and a thermocouple was used to measure the inside temperature. We used various cord lengths during bending (concave down) and compression (concave upward) to measure the change of resistance of rGO-coated yarns (10 cm length). A Zwick/Roell tensile tester (Zwick Roell Group, Germany) was used to control the cord length during bending and compression tests in both the forward and reverse directions. The change of the resistance with the change of cord lengths of rGO-coated yarns during bending and compression was captured using a National Instrument 9219 data acquisition card (NI, American).

ASSOCIATED CONTENT

Supporting Information

The Supporting Information is available free of charge on the ACS Publications website at DOI: 10.1021/acsnano.9b00319.

Additional figures and information (PDF)

AUTHOR INFORMATION

Corresponding Authors

*E-mail: mdnazmul.karim@manchester.ac.uk.
*E-mail: kostya@manchester.ac.uk.

ORCID

Nazmul Karim: 0000-0002-4426-8995

Author Contributions

N.K. and S.A. contributed equally to this work as joint first author. N.K. and K.S.N. conceived and designed the experiments. S.A. developed the inks with the help of N.K. and conducted all experiments. D.G. and Z.W. performed electrical transport measurements. D.G. analyzed electrical transport measurements data. P.H. carried out measurements of knitted temperature sensor. A.F. modeled, designed, and fabricated knitted sensors. S.T. carried out the flexibility measurements. N.K., S.A., and K.S.N. wrote the manuscript and Supporting Information. All other authors contributed to the manuscript.

Notes

The authors declare no competing financial interest.

ACKNOWLEDGMENTS

The authors kindly acknowledge the Government of Bangladesh for Ph.D. funding of S.A. This work was supported by EU Graphene Flagship Program, European Research Council Synergy Grant Hetero2D, the Royal Society, and Engineering and Physical Sciences Research Council, U.K. (EPSRC Grant No. EP/N010345/1, 2015). The authors also kindly acknowledge Kazi Farhan Hossain Purba for help with the graphics and Dr. Khalid Omari for useful discussions.

REFERENCES

(1) Bariya, M.; Nyein, H. Y. Y.; Javey, A. Wearable Sweat Sensors. *Nat. Electron.* **2018**, *1*, 160−171.

(2) Son, D.; Lee, J.; Qiao, S.; Ghaffari, R.; Kim, J.; Lee, J. E.; Song, C.; Kim, S. J.; Lee, D. J.; Jun, S. W.; Yang, S.; Park, M.; Shin, J.; Do, K.; Lee, M.; Kang, K.; Hwang, C. S.; Lu, N.; Hyeon, T.; Kim, D. H. Multifunctional Wearable Devices for Diagnosis and Therapy of Movement Disorders. *Nat. Nanotechnol.* **2014**, *9*, 397−404.

(3) Rogers, J. A. Nanomesh On-Skin Electronics. *Nat. Nanotechnol.* **2017**, *12*, 839−840.

(4) Abdelkader, A. M.; Karim, N.; Vallés, C.; Afroj, S.; Novoselov, K. S.; Yeates, S. G. Ultraflexible and Robust Graphene Supercapacitors Printed on Textiles for Wearable Electronics Applications. *2D Mater.* **2017**, *4*, 035016.

(5) Yetisen, A. K.; Qu, H.; Manbachi, A.; Butt, H.; Dokmeci, M. R.; Hinestroza, J. P.; Skorobogatiy, M.; Khademhosseini, A.; Yun, S. H. Nanotechnology in Textiles. *ACS Nano* **2016**, *10*, 3042−3068.

(6) Karim, N.; Afroj, S.; Tan, S.; He, P.; Fernando, A.; Carr, C.; Novoselov, K. S. Scalable Production of Graphene-Based Wearable E-Textiles. *ACS Nano* **2017**, *11*, 12266−12275.

(7) Karim, N.; Afroj, S.; Malandraki, A.; Butterworth, S.; Beach, C.; Rigout, M.; Novoselov, K.; Casson, A. J.; Yeates, S. All Inkjet-Printed Graphene-Based Conductive Pattern for Wearable E-Textiles Application. *J. Mater. Chem. C* **2017**, *5*, 11640−11648.

(8) Rodgers, M. M.; Pai, V. M.; Conroy, R. S. Recent Advances in Wearable Sensors for Health Monitoring. *IEEE Sens. J.* **2015**, *15*, 3119−3126.

(9) Xu, L.; Yang, G.; Jing, H.; Wei, J.; Han, Y. Ag−Graphene Hybrid Conductive Ink for Writing Electronics. *Nanotechnology* **2014**, *25*, 055201.

(10) Irimia-Vladu, M.; Głowacki, E. D.; Voss, G.; Bauer, S.; Sariciftci, N. S. Green and Biodegradable Electronics. *Mater. Today* **2012**, *15*, 340−346.

(11) Zeng, W.; Shu, L.; Li, Q.; Chen, S.; Wang, F.; Tao, X. M. Fiber-Based Wearable Electronics: A Review of Materials, Fabrication, Devices, and Applications. *Adv. Mater.* **2014**, *26*, 5310−5336.

(12) Gillooly, J. F.; Brown, J. H.; West, G. B.; Savage, V. M.; Charnov, E. L. Effects of Size and Temperature on Metabolic Rate. *Science* **2001**, *293*, 2248−2251.

(13) Parikshit, S.; Sampath Kumar, P.; Vadali, V. S. S. S.; Sushmee, B. Graphene-Based Wearable Temperature Sensor and Infrared Photodetector on A Flexible Polyimide Substrate. *Flex. Print. Electron.* **2016**, *1*, 025006.

(14) Cravero, J. P. Thermoregulation: Hypothermia and Hyperthermia. *Pediatr. Anesth. Rev.* **2017**, 667−680.

(15) Kurz, A.; Sessler, D. I.; Lenhardt, R. Perioperative Normothermia to Reduce the Incidence of Surgical-Wound Infection and Shorten Hospitalization. *N. Engl. J. Med.* **1996**, *334*, 1209−1216.

(16) Triffterer, L.; Marhofer, P.; Sulyok, I.; Keplinger, M.; Mair, S.; Steinberger, M.; Klug, W.; Kimberger, O. Forced-Air Warming During Pediatric Surgery: A Randomized Comparison of a Compressible with a Noncompressible Warming System. *Anesth. Analg.* **2016**, *122*, 219−225.

(17) Schmied, H.; Kurz, A.; Sessler, D. I.; Kozek, S.; Reiter, A. Mild Hypothermia Increases Blood Loss and Transfusion Requirements During Total Hip Arthroplasty. *Lancet* **1996**, *347*, 289−92.

(18) Lenhardt, R.; Marker, E.; Goll, V.; Tschernich, H.; Kurz, A.; Sessler, D. I.; Narzt, E.; Lackner, F. Mild Intraoperative Hypothermia Prolongs Postanesthetic Recovery. *Anesthesiology* **1997**, *87*, 1318−23.

(19) Thomsen, J. H.; Nielsen, N.; Hassager, C.; Wanscher, M.; Pehrson, S.; Køber, L.; Bro-Jeppesen, J.; Søholm, H.; Winther-Jensen, M.; Pellis, T.; Kuiper, M.; Erlinge, D.; Friberg, H.; Kjaergaard, J. Bradycardia During Targeted Temperature Management: An Early

DOI: 10.1021/acsnano.9b00319
ACS Nano 2019, 13, 3847−3857

Marker of Lower Mortality and Favorable Neurologic Outcome in Comatose Out-of-Hospital Cardiac Arrest Patients. *Crit. Care Med.* **2016**, *44*, 308−318.
(20) Jingjie, F.; Congcong, Z.; Cheng, H.; Yuan, L.; Xuesong, Y. Development of An Improved Wearable Device for Core Body Temperature Monitoring Based on the Dual Heat Flux Principle. *Physiol. Meas.* **2017**, *38*, 652.
(21) Mansor, H.; Shukor, M. H. A.; Meskam, S. S.; Rusli, N. Q. A. M.; Zamery, N. S. In *Body Temperature Measurement for Remote Health Monitoring System*, 2013 IEEE International Conference on Smart Instrumentation, Measurement and Applications (ICSIMA), Nov 25−27 , 2013; pp 1−5.
(22) Parikshit, S.; Sushmee, B. Eraser-Based Eco-Friendly Fabrication of a Skin-Like Large-Area Matrix of Flexible Carbon Nanotube Strain and Pressure Sensors. *Nanotechnology* **2017**, *28*, 095501−095510.
(23) Soukup, R.; Hamacek, A.; Mracek, L.; Reboun, J. In *Textile Based Temperature and Humidity Sensor Elements for Healthcare Applications*, Proceedings of the 2014 37th International Spring Seminar on Electronics Technology, May 7−11, 2014; pp 407−411.
(24) Kinkeldei, T.; Zysset, C.; Cherenack, K.; Troester, G. In *Development and Evaluation of Temperature Sensors for Textile Integration*, 2009 IEEE Sens J, Oct 25−28, 2009; pp 1580−1583.
(25) Novoselov, K. S.; Geim, A. K.; Morozov, S. V.; Jiang, D.; Zhang, Y.; Dubonos, S. V.; Grigorieva, I. V.; Firsov, A. A. Electric Field Effect in Atomically Thin Carbon Films. *Science* **2004**, *306*, 666−669.
(26) Geim, A. K. Graphene: Status and Prospects. *Science* **2009**, *324*, 1530−1534.
(27) He, Q.; Wu, S.; Yin, Z.; Zhang, H. Graphene-Based Electronic Sensors. *Chem. Sci.* **2012**, *3*, 1764−1772.
(28) Balandin, A. A.; Ghosh, S.; Bao, W.; Calizo, I.; Teweldebrhan, D.; Miao, F.; Lau, C. N. Superior Thermal Conductivity of Single-Layer Graphene. *Nano Lett.* **2008**, *8*, 902−907.
(29) Sun, P.; Zhu, M.; Wang, K.; Zhong, M.; Wei, J.; Wu, D.; Zhu, H. Small Temperature Coefficient of Resistivity of Graphene/Graphene Oxide Hybrid Membranes. *ACS Appl. Mater. Interfaces* **2013**, *5*, 9563−9571.
(30) Shateri-Khalilabad, M.; Yazdanshenas, M. E. Fabricating Electroconductive Cotton Textiles Using Graphene. *Carbohydr. Polym.* **2013**, *96*, 190−195.
(31) Yun, Y. J.; Hong, W. G.; Kim, W. J.; Jun, Y.; Kim, B. H. A Novel Method for Applying Reduced Graphene Oxide Directly to Electronic Textiles from Yarns to Fabrics. *Adv. Mater.* **2013**, *25*, 5701−5705.
(32) Davaji, B.; Cho, H. D.; Malakoutian, M.; Lee, J. K.; Panin, G.; Kang, T. W.; Lee, C. H. A Patterned Single Layer Graphene Resistance Temperature Sensor. *Sci. Rep.* **2017**, *7*, 8811−8820.
(33) Lee, H.; Choi, T. K.; Lee, Y. B.; Cho, H. R.; Ghaffari, R.; Wang, L.; Choi, H. J.; Chung, T. D.; Lu, N.; Hyeon, T.; Choi, S. H.; Kim, D. H. A Graphene-Based Electrochemical Device with Thermoresponsive Microneedles for Diabetes Monitoring and Therapy. *Nat. Nanotechnol.* **2016**, *11*, 566−572.
(34) Sun, Q.; Sun, X.; Jia, W.; Xu, Z.; Luo, H.; Liu, D.; Zhang, L. Graphene-Assisted Microfiber for Optical-Power-Based Temperature Sensor. *IEEE Photonics Technol. Lett.* **2016**, *28*, 383−386.
(35) Ayán-Varela, M.; Paredes, J. I.; Villar-Rodil, S.; Rozada, R.; Martínez-Alonso, A.; Tascón, J. M. D. A Quantitative Analysis of the Dispersion Behavior of Reduced Graphene Oxide in Solvents. *Carbon* **2014**, *75*, 390−400.
(36) Liu, J.; Tang, J.; Gooding, J. J. Strategies for Chemical Modification of Graphene and Applications of Chemically Modified Graphene. *J. Mater. Chem.* **2012**, *22*, 12435−12452.
(37) Hummers, W. S.; Offeman, R. E. Preparation of Graphitic Oxide. *J. Am. Chem. Soc.* **1958**, *80*, 1339−1339a.
(38) Su, Y.; Kravets, V. G.; Wong, S. L.; Waters, J.; Geim, A. K.; Nair, R. R. Impermeable Barrier Films and Protective Coatings Based on Reduced Graphene Oxide. *Nat. Commun.* **2014**, *5*, 4843.
(39) Dao, T. D.; Lee, H. I.; Jeong, H. M.; Kim, B. K. Direct Covalent Modification of Thermally Exfoliated Graphene Forming Functionalized Graphene Stably Dispersible in Water and Poly (Vinyl Alcohol). *Colloid Polym. Sci.* **2013**, *291*, 2365−2374.
(40) Karim, N.; Zhang, M.; Afroj, S.; Koncherry, V.; Potluri, P.; Novoselov, K. S. Graphene-Based Surface Heater for De-Icing Applications. *RSC Adv.* **2018**, *8*, 16815−16823.
(41) Sarker, F.; Karim, N.; Afroj, S.; Koncherry, V.; Novoselov, K. S.; Potluri, P. High-Performance Graphene-Based Natural Fiber Composites. *ACS Appl. Mater. Interfaces* **2018**, *10*, 34502−34512.
(42) Johnson, D. W.; Dobson, B. P.; Coleman, K. S. A Manufacturing Perspective On Graphene Dispersions. *Curr. Opin. Colloid Interface Sci.* **2015**, *20*, 367−382.
(43) Joung, D.; Khondaker, S. I. Efros-Shklovskii Variable-Range Hopping in Reduced Graphene Oxide Sheets of Varying Carbon sp^2 Fraction. *Phys. Rev. B: Condens. Matter Mater. Phys.* **2012**, *86*, 235423.
(44) Park, M.; Hong, S. J.; Kim, K. H.; Kang, H.; Lee, M.; Jeong, D. H.; Park, Y. W.; Kim, B. H. Electrical and Thermoelectric Transport by Variable Range Hopping in Reduced Graphene Oxide. *Appl. Phys. Lett.* **2017**, *111*, 173103.
(45) Abdelkader, A. M.; Patten, H. V.; Li, Z.; Chen, Y.; Kinloch, I. A. Electrochemical Exfoliation of Graphite in Quaternary Ammonium-Based Deep Eutectic Solvents: A Route for the Mass Production of Graphane. *Nanoscale* **2015**, *7*, 11386−11392.
(46) Swain, A. K.; Bahadur, D. Enhanced Stability of Reduced Graphene Oxide Colloid Using Cross-Linking Polymers. *J. Phys. Chem. C* **2014**, *118*, 9450−9457.
(47) Zhang, J.; Yang, H.; Shen, G.; Cheng, P.; Zhang, J.; Guo, S. Reduction of Graphene Oxide *via* L-Ascorbic Acid. *Chem. Commun.* **2010**, *46*, 1112−1114.
(48) Tiannan, Z.; Feng, C.; Kai, L.; Hua, D.; Qin, Z.; Jiwen, F.; Qiang, F. A Simple and Efficient Method to Prepare Graphene by Reduction of Graphite Oxide with Sodium Hydrosulfite. *Nanotechnology* **2011**, *22*, 045704.
(49) Atalay, O.; Kennon, W. R.; Husain, M. D. Textile-Based Weft Knitted Strain Sensors: Effect of Fabric Parameters on Sensor Properties. *Sensors* **2013**, *13*, 11114−11127.
(50) Juan, X.; Hairu, L.; Menghe, M. High Sensitivity Knitted Fabric Strain Sensors. *Smart Mater. Struct.* **2016**, *25*, 105008.
(51) Boland, C. S.; Khan, U.; Backes, C.; O'Neill, A.; McCauley, J.; Duane, S.; Shanker, R.; Liu, Y.; Jurewicz, I.; Dalton, A. B.; Coleman, J. N. Sensitive, High-Strain, High-Rate Bodily Motion Sensors Based on Graphene−Rubber Composites. *ACS Nano* **2014**, *8*, 8819−8830.
(52) Seyedin, S.; Razal, J. M.; Innis, P. C.; Jeiranikhameneh, A.; Beirne, S.; Wallace, G. G. Knitted Strain Sensor Textiles of Highly Conductive All-Polymeric Fibers. *ACS Appl. Mater. Interfaces* **2015**, *7*, 21150−21158.
(53) Gao, Y.; Shi, W.; Wang, W.; Leng, Y.; Zhao, Y. Inkjet Printing Patterns of Highly Conductive Pristine Graphene on Flexible Substrates. *Ind. Eng. Chem. Res.* **2014**, *53*, 16777−16784.
(54) Xu, W.; Li, Y. Cotton Fabric Strength Loss From Treatment With Polycarboxylic Acids for Durable Press Performance. *Text. Res. J.* **2000**, *70*, 957−961.
(55) Karim, M. N.; Rigout, M.; Yeates, S. G.; Carr, C. Surface Chemical Analysis of the Effect of Curing Conditions on the Properties of Thermally-Cured Pigment Printed Poly (Lactic Acid) Fabrics. *Dyes Pigm.* **2014**, *103*, 168−174.
(56) Maiti, U. N.; Maiti, S.; Das, N. S.; Chattopadhyay, K. K. Hierarchical Graphene Nanocones over 3D Platform of Carbon Fabrics: A Route Towards Fully Foldable Graphene Based Electron Source. *Nanoscale* **2011**, *3*, 4135−4141.
(57) Ju Yun, Y.; Hong, W. G.; Choi, N. J.; Hoon Kim, B.; Jun, Y.; Lee, H. K. Ultrasensitive and Highly Selective Graphene-Based Single Yarn for Use in Wearable Gas Sensor. *Sci. Rep.* **2015**, *5*, 10904.
(58) Kong, D.; Le, L. T.; Li, Y.; Zunino, J. L.; Lee, W. Temperature-Dependent Electrical Properties of Graphene Inkjet-Printed on Flexible Materials. *Langmuir* **2012**, *28*, 13467−13472.
(59) Sahoo, S.; Barik, S. K.; Sharma, G.; Khurana, G.; Scott, J.; Katiyar, R. S. Reduced Graphene Oxide as Ultra-Fast Temperature Sensor. *arXiv preprint arXiv:1204.1928*, **2012**.

DOI: 10.1021/acsnano.9b00319
ACS Nano 2019, 13, 3847−3857

(60) Cook, B. S.; Vyas, R.; Kim, S.; Thai, T.; Le, T.; Traille, A.; Aubert, H.; Tentzeris, M. M. RFID-Based Sensors for Zero-Power Autonomous Wireless Sensor Networks. *IEEE Sens. J.* **2014**, *14*, 2419−2431.
(61) Choperena, M. RFID-powered Sensors Can Play a Big Role in the Internet of Things. http://www.rfidjournal.com/articles/view?11062 (accessed 02/12/2017).

DOI: 10.1021/acsnano.9b00319
ACS Nano 2019, 13, 3847−3857